Key Points:
- Seven hydrologic models were intercompared on standard benchmark problems
- In general, though there are differences in approach, these models agree
- Model differences can be attributed to solution technique and coupling strategy

Correspondence to:
R. M. Maxwell,
rmaxwell@mines.edu

Surface-subsurface model intercomparison: A first set of benchmark results to diagnose integrated hydrology and feedbacks

Reed M. Maxwell[1], Mario Putti[2], Steven Meyerhoff[1], Jens-Olaf Delfs[3,4], Ian M. Ferguson[1,5], Valeriy Ivanov[6], Jongho Kim[6], Olaf Kolditz[3,7], Stefan J. Kollet[8], Mukesh Kumar[9], Sonya Lopez[1], Jie Niu[10], Claudio Paniconi[11], Young-Jin Park[12], Mantha S. Phanikumar[10], Chaopeng Shen[13], Edward A. Sudicky[12], and Mauro Sulis[14]

[1]Integrated GroundWater Modeling Center and Department of Geology and Geological Engineering, Colorado School of Mines, Golden, Colorado, USA, [2]Department of Mathematics, University of Padova, Padova, Italy, [3]Helmholtz Centre for Environmental Research UFZ, Leipzig, Germany, [4]Water-Earth Systems Science (WESS), Center for Applied Geoscience, Tübingen, Germany, [5]Technical Services Center, US Bureau of Reclamation, Lakewood, Colorado, USA, [6]Department of Civil and Environmental Engineering, University of Michigan, Ann Arbor, Michigan, USA, [7]Technical University of Dresden, Environmental Sciences, Dresden, Germany, [8]Centre for High-Performance Scientific Computing in Terrestrial Systems, HPSC TerrSys, Institute for Bio- and Geosciences, Agrosphere (IBG-3), Research Centre Jülich, Jülich, Germany, [9]Nicholas School of the Environment, Duke University, Durham, North Carolina, USA, [10]Department of Civil and Environmental Engineering, Michigan State University, East Lansing, Michigan, USA, [11]Institut National de la Recherche Scientifique, Centre Eau Terre Environnement, Quebec City, Quebec, Canada, [12]Department of Earth and Environmental Sciences, University of Waterloo, Waterloo, Ontario, Canada, [13]Department of Civil and Environmental Engineering, Pennsylvania State University, University Park, Pennsylvania, USA, [14]Meteorological Institute, Bonn University, Bonn, Germany

Abstract There are a growing number of large-scale, complex hydrologic models that are capable of simulating integrated surface and subsurface flow. Many are coupled to land-surface energy balance models, biogeochemical and ecological process models, and atmospheric models. Although they are being increasingly applied for hydrologic prediction and environmental understanding, very little formal verification and/or benchmarking of these models has been performed. Here we present the results of an intercomparison study of seven coupled surface-subsurface models based on a series of benchmark problems. All the models simultaneously solve adapted forms of the Richards and shallow water equations, based on fully 3-D or mixed (1-D vadose zone and 2-D groundwater) formulations for subsurface flow and 1-D (rill flow) or 2-D (sheet flow) conceptualizations for surface routing. A range of approaches is used for the solution of the coupled equations, including global implicit, sequential iterative, and asynchronous linking, and various strategies are used to enforce flux and pressure continuity at the surface-subsurface interface. The simulation results show good agreement for the simpler test cases, while the more complicated test cases bring out some of the differences in physical process representations and numerical solution approaches between the models. Benchmarks with more traditional runoff generating mechanisms, such as excess infiltration and saturation, demonstrate more agreement between models, while benchmarks with heterogeneity and complex water table dynamics highlight differences in model formulation. In general, all the models demonstrate the same qualitative behavior, thus building confidence in their use for hydrologic applications.

1. Introduction

Hydrology is increasingly becoming integrated and interdisciplinary. There are a growing number of hydrologic models, coupled and integrated, being used to address a range of science questions. These models couple surface and subsurface flow with the aim of representing the relevant physical processes influencing the hydrologic response at scales ranging from small catchments to large river basins. They implement a different set of one, two, and fully three-dimensional representations and numerical solution techniques as well as a variety of methodologies for coupling different hydrologic processes. Additionally, these hydrologic models are being coupled to land-surface energy, biogeochemistry/ecology, dynamic vegetation, solute transport, and atmospheric models [e.g., *VanderKwaak and Loague*, 2001; *Bixio et al.*, 2002; *Panday and Huyakorn*, 2004; *Maxwell and Miller*, 2005; *Kollet and Maxwell*, 2006; *Maxwell et al.*, 2007; *Ivanov et al.*, 2008; *Kollet and Maxwell*, 2008a; *Maxwell et al.*, 2011; *Weill et al.*, 2011; *Niu et al.*, 2014].

Despite the fact that several different coupled models have been developed, very few analytical solutions have been published [e.g., *Parlange et al.*, 1981] and no coupled surface-subsurface analytical solutions are known. Thus, even verifying these models (i.e., ensuring their numerical solutions are accurate) is a challenge. In the absence of exact solutions, a common verification approach is to compare model results against other published solutions [e.g., *Panday and Huyakorn*, 2004; *Kollet and Maxwell*, 2006; *Shen and Phanikumar*, 2010; *Sulis et al.*, 2010; *Sebben et al.*, 2013], but standard procedures and benchmark test cases for coupled surface-subsurface models have not yet been established.

Within the fields of hydrology and land-surface processes, two prior successful intercomparison exercises should be highlighted. These are the Project for Intercomparison of Land-Surface Parameterization Schemes (PILPS) and the Distributed Model Intercomparison Project (DMIP). PILPS [e.g., *Henderson-Sellers et al.*, 1995; *Yang et al.*, 1995; *Chen et al.*, 1997; *Qu et al.*, 1998; *Liang et al.*, 1998; *Luo et al.*, 2003] classified a number of land-surface models based on formulation and conducted several intercomparison studies using synthetic and real sites over a range of climatologies. DMIP [*Reed et al.*, 2004; *Smith et al.*, 2004] tested distributed hydrologic models against one another and against simpler, lumped models over several real sites in North America.

In this paper, we present the results of the first intercomparison performed specifically for integrated hydrologic models. We classify these models based on their formulation, include models with more simplified physics, and intercompare them using idealized test cases. This intercomparison is the first in a series of exercises that will grow in complexity to eventually include real sites. Here we distinguish between integrated, or coupled, hydrologic models that solve the surface and subsurface flow equations in a combined fashion using numerical solution techniques in a spatially explicit manner (for further expansion on these definitions, see *Condon and Maxwell* [2013]) and models that simplify these processes. The models are capable of resolving feedbacks and interactions between surface and subsurface flow. All the models tested here ensure a complete balance of water between the surface and subsurface systems and are thus mass conservative. The idealized problems that are used as test cases emphasize the role of various model components and their interactions. These benchmark problems are used to compare the flow components of seven integrated hydrologic models: CATHY, HydroGeo-Sphere (HGS), OpenGeoSys (OGS), ParFlow, PAWS, PIHM, and tRIBS + VEGGIE, which are all described in detail later. This study extends the work of *Sulis et al.* [2010] in which two of these models (CATHY and ParFlow) were assessed. The guiding principle of this work is that a set of different integrated hydrologic models can be run on standardized benchmark problems by a community of model developers, generating an increased understanding of the representation of coupled hydrologic processes and insights into the differences and similarities in the simulation results. The benchmark problems, together with model solutions and results, are provided freely to the hydrologic community so that the initiative can be extended to any other model or modeling approach. The benchmarks start with simple cases and increase in complexity. Because we do not know the correct solution to these cases we can only discuss model differences, and by providing these benchmarks we can build confidence in the use of integrated hydrologic models.

2. Background

A blueprint for modeling fully integrated surface, subsurface, and land-surface processes that was originally put forth 45 years ago [*Freeze and Harlan*, 1969] is now becoming a reality. Although truly fully coupled models have only recently appeared in the literature [e.g., *VanderKwaak and Loague*, 2001; *Bixio et al.*, 2002; *Panday and Huyakorn*, 2004; *Jones et al.*, 2006; *Kollet and Maxwell*, 2006; *Qu and Duffy*, 2007; *Kollet and Maxwell*, 2008a], there is now a growing library of models and a community of modelers that contribute considerably to our understanding of the coupled terrestrial hydrologic and energy cycles. Advances in numerical and computational technologies have, in part, enabled new approaches for modeling these coupled interactions. While these models all take different numerical, discretization, and even coupling approaches, they all share the common goal to rigorously, mathematically model the terrestrial hydrologic and energy cycle as an integrated system. Research addressing these issues encompasses a range of scales and includes a variety of processes. Table 1 provides a survey of the range of applications and study of coupled models [after *Ebel et al.*, 2009].

A key component to the integrated blueprint is the coupled solution of Richards' equation [*Richards*, 1931] and the Saint Venant equations, which are briefly presented below. A standard formulation of the Richards equation that includes also groundwater (saturated zone) flow is:

Table 1. Survey of Integrated Hydrologic Modeling Studies (Modified From *Ebel et al.* [2009])

Focus	Reference(s)
Agricultural sustainability	*Schoups et al.* [2005]
Atmosphere-subsurface water and energy fluxes	*Maxwell and Miller* [2005] *Maxwell et al.* [2007, 2011] *Kollet and Maxwell* [2008a] *Maxwell and Kollet* [2008a] *Niu et al.* [2014]
Climate change impacts/feedbacks	*Maxwell and Kollet* [2008a] *Ferguson and Maxwell* [2010] *Sulis et al.* [2011a, 2012]
Dam removal	*Heppner and Loague* [2008] *Li and Duffy* [2011]
Groundwater recharge	*Lemieux et al.* [2008] *Markstrom et al.* [2008] *Smerdon et al.* [2008] *Guay et al.* [2013]
Groundwater-lake interaction	*Smerdon et al.* [2007] *Hunt et al.* [2008]
New-old water/residence times	*VanderKwaak and Sudicky* [2000] *Jones et al.* [2006] *Cardenas et al.* [2008] *Cardenas* [2008a, 2008b] *Kollet and Maxwell* [2008b]
Pore-water pressure development and slope instability	*Ebel et al.* [2007] *Mirus et al.* [2007] *Ebel and Loague* [2008] *Ebel et al.* [2008]
Radionuclide contamination/vulnerability	*McLaren et al.* [2000] *Bixio et al.* [2002]
Runoff generation	*VanderKwaak and Loague* [2001] *Morita and Yen* [2002] *Loague et al.* [2005] *Kollet and Maxwell* [2006] *Ebel et al.* [2007, 2008] *Heppner et al.* [2007] *Qu and Duffy* [2007] *Jones et al.* [2008] *Li et al.* [2008] *Maxwell and Kollet* [2008b] *Mirus et al.* [2009] *Camporese et al.* [2009] *Gauthier et al.* [2009] *Sulis et al.* [2011b] *Meyerhoff and Maxwell* [2011] *Delfs et al.* [2013]
Sediment transport	*Heppner et al.* [2006] *Heppner et al.* [2007] *Ran et al.* [2007] *Li and Duffy* [2011]
Solute transport	*VanderKwaak and Sudicky* [2000] *Ebel et al.* [2007] *Sudicky et al.* [2008] *Weill et al.* [2011]
Stream-aquifer exchange	*Weng et al.* [1999] *Gunduz and Aral* [2003, 2005] *Cardenas* [2008a, 2008b] *Brookfield et al.* [2008] *Cardenas and Gooseff* [2008] *Peyrard et al.* [2008] *Frei et al.* [2009]
Wetland-estuary exchange	*Langevin et al.* [2005]
Urban systems	*Delfs et al.* [2012]

$$S_s S_w(h) \frac{\partial h}{\partial t} + \phi \frac{\partial S_w(h)}{\partial t} = \nabla \cdot \boldsymbol{q} + q_s + q_e/m' \tag{1}$$

where the specific volumetric (Darcy) flux is denoted by q [LT^{-1}]:

$$\boldsymbol{q} = -\boldsymbol{K_s} k_r(h) \nabla(h-z) \tag{2}$$

In these expressions, h is the pressure head [L], z is the vertical coordinate [L] (positive downward), $\boldsymbol{K_s}$ is the saturated hydraulic conductivity tensor [LT^{-1}], k_r is the relative permeability [-], S_s is the specific storage coefficient [L^{-1}], ϕ is the porosity [-], S_w is the relative saturation [-] (often written as the soil moisture or volumetric water content θ divided by the saturated moisture content, the latter usually assumed to be equal to the porosity), q_s is a general source/sink term that might represent pumping or injection [T^{-1}], q_e is a general source/sink term that represents exchange fluxes [LT^{-1}], and m' is an interfacial thickness [L].

The nonlinear functions for the relative hydraulic conductivity $k_r(h)$ and water saturation $S_w(h)$ can be specified using, for example, the *van Genuchten* [1980] or *Brooks and Corey* [1964] relationships, or in tabular form.

Mass conservation for overland flow is:

$$\frac{\partial h}{\partial t} = \nabla \cdot (\boldsymbol{v}h) + q_e(x) + q_r(x) \tag{3}$$

where $q_e(x)$ represents exchange fluxes between surface and subsurface domains, $q_r(x)$ is a general source/sink term [LT^{-1}], and x is a general spatial coordinate [L]. Manning's equation is often used to establish a flow depth-discharge relationship (though other approaches exist and can be implemented in place of Manning's), where the velocity vector $\boldsymbol{v}$ in (3) may be written as follows:

$$v_x^{sw} = \sqrt{\frac{S_{f,x}}{n}} h^{2/3} \quad \text{and} \quad v_y^{sw} = \sqrt{\frac{S_{f,y}}{n}} h^{2/3} \tag{4}$$

where $S_{f,i}$ [L] is the friction slope, i stands for the x and y direction, and n [TL$^{-1/3}$] is Manning's coefficient.

3. Brief Description of Hydrologic Models

All the models we consider are based on adapted forms of the Richards equation describing flow in variably saturated porous media coupled to some form of the hydrostatic shallow water (i.e., Saint Venant) equations for surface flow routing. The differences between the seven models are due to various features, of which the most important are: (i) formulation of the governing equations (including dimensionality); (ii) interface boundary conditions that enforce at least pressure and mass flux continuity at the surface/subsurface interface; and (iii) numerical approaches for spatial and temporal discretization and coupling. For surface flow, the shallow water equations are solved in either one dimension (rill flow conceptualization) or two (sheet flow conceptualization), while for subsurface flow Richards' equation is solved in either three dimensions or it is simplified vertically (1-D) for the vadose zone and coupled to a 2-D linear groundwater flow equation.

Coupled hydrologic models can be classified according to solution technique or according to coupling strategy. We can define three approaches for solving the coupled system of equations (1) and (3): asynchronous linking, sequential iteration, and globally implicit [*Panday and Huyakorn*, 2004; *Furman*, 2008; *Park et al.*, 2009; *Dagès et al.*, 2012]. The first strategy progresses in time by lagging the dependent variables so that different governing equations can be solved asynchronously. The second procedure can be identified as a time-splitting methodology by which the lagged variables are used to define a functional iteration that is carried out until convergence. Finally, globally implicit schemes cast all the variables in a single nonlinear system of equations.

In terms of coupling strategy, there are three distinct formulations for integrating hydrostatic surface and subsurface flow: first-order exchange [e.g., *VanderKwaak and Loague*, 2001; *Panday and Huyakorn*, 2004;

Table 2. Classification of the Surface-Subsurface Hydrologic Models Used in the Intercomparison Study

Model	Solution Technique	Coupling Strategy	Grid
CATHY	BC Switching	Sequential iterative	Unstructured
HydroGeoSphere	First-order exchange[a]	Global implicit	Unstructured[b]
OGS	First-order exchange	Sequential iterative	Unstructured
PIHM	First-order exchange	Global implicit	Unstructured
ParFlow	Pressure continuity	Global implicit	Structured[c]
PAWS	First-order exchange	Asynchronous linking	Structured
tRIBS − VEGGIE	First-order exchange	Asynchronous linking	Unstructured

[a]Can simulate both pressure continuity and first-order exchange, only first-order exchange used for this study.
[b]Can use both structured and unstructured grids, only unstructured grid used for this study.
[c]Has some semistructured grid capabilities, only structured grid used for this study.

Therrien et al., 2012], continuity of pressure [e.g., *Kollet and Maxwell*, 2006; *Dawson*, 2008; *Therrien et al.*, 2012], and boundary condition switching [e.g., *Camporese et al.*, 2010]. We note here that the complexity of the physical phenomena involved in the formulations and their numerical representations mandates simplifications which are adopted to varying extents in the different models. While all the approaches aim at maintaining pressure and flux continuity at the surface/subsurface interface, a common hypothesis is to neglect continuity of momentum (and thus forces). The seven models used in the intercomparison use either structured or unstructured meshes for the discretization of the Richards and Saint Venant equations. Unstructured grids offer flexibility in handling complex features while structured grids offer advantages in computational simplicity and are more amenable to efficient parallelization. A brief description of each of the seven models is given in the following subsections, and a classification summary is provided in Table 2.

3.1. CATHY

CATHY (CATchment HYdrology) [*Bixio et al.*, 2002; *Camporese et al.*, 2010] combines a finite element approach for the three-dimensional Richards equation (1) with a finite difference discretization of a path-based 1-D kinematic wave equation, coupled via a time-splitting based sequential iterative procedure. A diffusion term is introduced in the kinematic wave equation using the Muskingum-Cunge (matched artificial diffusion or MAD) technique so that the numerical dispersion is used to represent hydrodynamic spreading. Surface and subsurface coupling is based on a boundary condition switching procedure that automatically partitions potential fluxes (rainfall and evapotranspiration) into actual fluxes across the landsurface, and calculates changes in surface storage. This procedure, which is performed at every subsurface time step, determines whether a surface node is ponded, saturated, unsaturated, or air dry, and it ensures that pressure and flux continuity is enforced at the surface/subsurface interface. A one-dimensional drainage network is computed from the catchment ground elevation [*Orlandini and Moretti*, 2009] and used to define the geometry for the solution of the Saint Venant equation. The surface module considers both hillslope (rivulet representation) and stream (channel representation) routing. Rivulet flow is assumed to occur over all surface cells for which the upstream drainage area does not exceed a predefined threshold value, while channel flow is assumed on all other cells. The numerical approximation of Richards' equation is based on tetrahedral finite elements combined with Euler time stepping and a Krylov-based Newton-type nonlinear solver with time step adaptation for ensuring convergence at every step [*Paniconi and Putti*, 1994]. In the surface routing solver, kinematic celerity and hydraulic diffusivity are calculated from the variable scaling parameters for the Manning coefficient and the water surface width [*Leopold and Maddock*, 1953; *Orlandini and Rosso*, 1998].

3.2. HydroGeoSphere

The HydroGeoSphere (HGS) model [*Aquanty Inc.*, 2013] is a three-dimensional control-volume finite element simulator designed to simulate the entire terrestrial portion of the hydrologic cycle. It uses a globally implicit approach to simultaneously solve the 2-D diffusive-wave equation and the 3-D form of Richards' equation (1). It also dynamically integrates key components of the hydrologic cycle such as evaporation from bare soil and water bodies, vegetation-dependent transpiration with root uptake, snowmelt, and soil freeze/thaw. Features such as macropores, fractures, and tile drains can either be incorporated discretely or using a dual-porosity, dual-permeability formulation. As with the solution of the coupled water flow equations, HydroGeoSphere solves the contaminant and energy transport equations over the land surface and

in the subsurface, thus allowing for surface/subsurface interactions. The HydroGeoSphere platform uses a Newton iteration to handle nonlinearities in the governing flow equations and a combined with an iterative sparse matrix solver.It has been parallelized to utilize high performance computing facilities to address large-scale problems.

3.3. OGS

OGS (OpenGeoSys) is an open-source platform for numerical simulation of coupled thermohydromechanical/chemical processes in porous and fractured media. The object-oriented finite element code is designed for applications in geomechanics, catchment hydrology, and energy research. Surface and subsurface flow are coupled by using the iterative sequential approach [*Delfs et al.*, 2009, 2012], while flow processes in a particular domain (e.g., two-phase, dual-porosity) are implicitly solved [*Delfs et al.*, 2013]. Diffusive-wave overland flow and the head-based form of the 3-D Richards equation (1) are discretized in space with an upwind control-volume and a standard (centered) Galerkin finite element method, respectively. The OGS community has created a broad spectrum of software interfaces to external flow and chemical simulators as well as for pre and postprocessing [*Kolditz et al.*, 2012].

3.4. ParFlow

ParFlow (Parallel Flow) is an open source, object-oriented simulation platform that solves the mixed form of the variably saturated Richards equation in three dimensions. Overland flow and groundwater-surface water interactions are represented through a free-surface overland flow boundary condition, which routes ponded water via the kinematic wave equation using a pressure-continuity condition [*Kollet and Maxwell*, 2006]. The coupled subsurface-overland equations are solved in a globally implicit manner using a highly efficient and robust Newton-Krylov method with multigrid preconditioning [*Ashby and Falgout*, 1996; *Jones and Woodward*, 2001], which exhibits excellent parallel scaling and allows simulation of large-scale, highly heterogeneous problems [*Kollet and Maxwell*, 2006; *Kollet et al.*, 2010; *Maxwell*, 2013]. Simultaneous solution ensures full interaction between surface and subsurface flows. ParFlow has been coupled to the Common Land Model (CLM) [*Maxwell and Miller*, 2005; *Kollet and Maxwell*, 2008b] which provides complete land-surface processes and to the Advanced Regional Prediction System (ARPS) [*Maxwell et al.*, 2007] and the Weather Research and Forecasting System (WRF) [*Maxwell et al.*, 2011) which provides coupling to the atmosphere.

3.5. PAWS

The PAWS (Process-based Adaptive Watershed Simulator) model [*Shen and Phanikumar*, 2010; *Shen et al.*, 2013] was developed to simulate hydrologic processes in large watersheds. To describe the integrated hydrologic response of the surface-subsurface system, PAWS uses asynchronous linking and couples the 1-D Richards equation for the vadose zone with a quasi 3-D Darcy (2-D unconfined and 3-D confined aquifer) model for the fully saturated domain. Grid cells on the land surface are connected to the groundwater domain through a string of 1-D cells that represent the vadose zone. Derived from applying simplifying assumptions to the 3-D Richards equation, the coupling scheme provides estimates of groundwater flow to the soil column. The last grid cell in the vadose zone, whose thickness can vary depending on the location of the phreatic water table, incorporates the dynamics of groundwater flow. The soil moisture profile obtained using this method is consistent with the groundwater head as described in *Shen and Phanikumar* [2010]. A mass balance equation is written for the ponding layer at the surface and the equation is solved simultaneously with soil water in the vadose zone using Picard iteration. The groundwater flow equations are solved using an iterative sparse matrix solver. Overland flow is described using the 2-D diffusive-wave equation, solved using a third-order total variation diminishing (TVD) Runge-Kutta scheme [*Shu*, 1988]. To enforce flux and pressure continuity at the interface between the surface ponding layer and soil water, the upper boundary condition for the Richards equation switches between a mass balance equation and a flux (Neumann-type) boundary condition depending on whether the ponding water will completely infiltrate in one time step.

3.6. PIHM

PIHM (Penn State Integrated Hydrologic Model) is a fully coupled, distributed hydrologic model for predicting states such as snow water equivalent, interception storage, overland flow depth, soil moisture, groundwater depth, and stream stage, and associated hydrologic fluxes such as streamflow, recharge, and

evapotranspiration [*Qu and Duffy*, 2007; *Kumar et al.*, 2009]. Here we use the next generation of PIHM (also referred to as FIHM) [*Kumar et al.*, 2009] that is second-order accurate in space and two to five order accurate in time, for solving unsteady diffusion wave overland and subsurface flow equations. A multidimensional linear reconstruction of the state gradients is used to achieve second-order spatial accuracy. The surface flow is based on a depth-averaged 2-D diffusive-wave approximation of the Saint Venant equations, while subsurface flow is based on the complete 3-D variably saturated form of Richards' equation. Full coupling between overland and vadose zone flow is based on continuity of head and flux. The spatial adaptability of the mesh elements and temporal adaptability of the numerical solver facilitates capture of multiple spatial and temporal scales by the model, while maintaining the conservation of mass at all cells (discretized unstructured mesh elements), as guaranteed by the finite volume formulation.

3.7. tRIBS + VEGGIE

The tRIBS (Triangulated Irregular Network (TIN)-Based Real Time Integrated Basin Simulator) is a distributed ecohydrologic model that considers hydrological processes such as rainfall interception, surface energy budget balance, evapotranspiration, infiltration, and runoff routing [*Ivanov et al.*, 2004]. Its updated version, tRIBS + VEGGIE + OFM [*Ivanov et al.*, 2008, 2010; *Kim et al.*, 2013], developed a vegetation dynamics module and incorporated a quasi 3-D framework to describe subsurface saturated-unsaturated zone dynamics. Specifically, a computational domain is represented using an unstructured mesh that undergoes Voronoi tessellation that identifies individual computational elements. At the scale of each element, the 1-D mixed formulation of the Richards equation is solved on a mesh in the direction normal to the surface. The numerical approximation is based on backward Euler time stepping and an implicit Picard iteration with time step adaptation [*Celia et al.*, 1990]. Galerkin-type linear finite elements are used to approximate variations within the mesh. The numerical scheme uses asynchronous coupling to the surface processes and mass exchanges modeled in the saturated zone. The saturated zone dynamics are resolved on an element-by-element basis using the same mesh and are based on the Boussinesq equation under the Dupuit-Forchheimer assumptions [*Bear*, 1979]. The flow direction in the subsurface saturated zone is determined using the D-infinity algorithm [*Tarboton*, 1997]. Lateral exchange in the unsaturated zone is gravity-driven only and the flow direction is also determined using the D-infinity method. tRIBS + VEGGIE has been coupled with the hydrodynamic overland flow model OFM [*Kim et al.*, 2012, 2013]. This model solves the full version of the 2-D Saint Venant equations. As compared to kinematic or inertia-free surface flow model formulations, tRIBS + VEGGIE + OFM resolves the Riemann problem caused by the different wave speeds by employing Roe's approximate finite volume solver on an unstructured triangular grid. The model simulates the entire domain, including hillslope and channel areas, in a seamless fashion and computes a solution of surface flow motion under the shallow water approximation.

4. Benchmark Simulation Cases

As is evident from the preceding descriptions, the seven models being considered in this study are based on different formulations of a variety of interlinked physical processes and different approximations for integration of the model components. Given this complexity, the mathematical properties and numerical behavior of each model are not yet fully understood and theoretical analysis to elucidate key differences between models is difficult. Numerical experiments therefore represent an essential tool for model intercomparison, and in this study simple experiments are used as a first step in exploring the similarities and differences between the seven models. The test cases involve simple geometries: a sloping plane and a tilted V-catchment [*Gottardi and Venutelli*, 1993; *Panday and Huyakorn*, 2004; *Kollet and Maxwell*, 2006; *Kumar et al.*, 2009; *Sulis et al.*, 2010] with minimal complexity in domain geometry and other features (topography, hydraulic and hydrogeological properties, and atmospheric forcing), but with complex physical responses designed to thoroughly compare model behavior. The test cases feature step functions of rainfall followed by a recession or evaporation period. The test cases also share common van Genuchten parameters based upon a sandy-loam soil from *Schaap and Leij* [1998]. The response variables analyzed include domain outflow, saturation conditions, and location of intersection between the water table and land surface. The simulations cases are: (1) infiltration excess, (2) saturation excess, (3) tilted V-catchment, (4) slab, and (5) return flow. A complete listing of all parameters is given in Table 3 and a summary of each case is provided below. While a comprehensive analysis of model run-time is outside the scope of this

Table 3. Parameter Values Used in the Test Cases

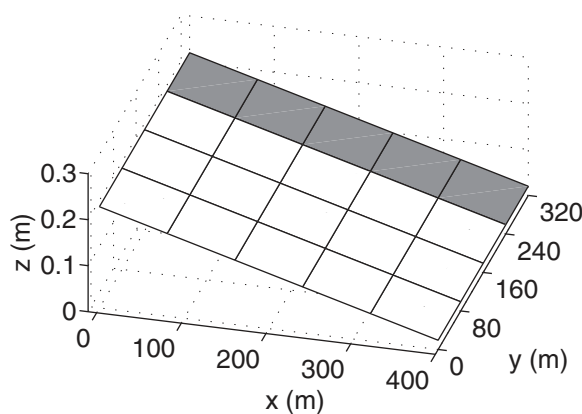|		Units	Parameter Values for Simulation Cases				
			1. Infiltration Excess	2. Saturation Excess	3. Tilted V-Catchment	4. Slab Case	5. Return Flow
Horizontal mesh size	$\Delta x = \Delta y$	m	80	80	20	1	5
Vertical mesh size	Δz	m	0.2	0.2	0.05	0.05	0.05
Initial water table depth	wt	M	1.0	1.0, 0.5	a	1.0	0.5
Saturated hydraulic conductivity	K_s	m min^{-1}	6.94×10^{-5}, 6.94×10^{-6}	6.94×10^{-4}	a	6.94×10^{-4} (Uniform) 6.94×10^{-6} (Slab)	6.94×10^{-2}
Specific storage	S_s	m^{-1}	5×10^{-4}	5×10^{-4}	5×10^{-4}	5×10^{-4}	5×10^{-4}
Porosity	φ		0.4	0.4	0.4	0.4	0.4
Mannings	n	m$^{-1/3}$ min	3.31×10^{-3}	3.31×10^{-3}	2.50×10^{-4} (Hillslope) 2.50×10^{-3} (Channel)	3.31×10^{-3}	3.31×10^{-3}
x direction slope		%	0.05	0.05	5 (Hillslope) 0 (Channel)	0.05	0.5, 5
y direction slope		%	0	0	2	0	0
Rain rate		m min^{-1}	3.30×10^{-4}	3.30×10^{-4}	1.80×10^{-4}	3.30×10^{-4}	1.50×10^{-4} 5.40×10^{-6}
Evaporation Rate[b]		m min^{-1}					
van Genuchten Parameters							
Alpha	a	cm^{-1}	1.0	1.0	1.0	1.0	1.0
Pore-size distributions	n	–	2.0	2.0	2.0	2.0	2.0
Residual water content	S_{res}	–	0.2	0.2	0.2	0.2	0.2
Saturated water content	S_{sat}	–	1.0	1.0	1.0	1.0	1.0

[a]Tilted V-Catchment case is surface flow only.
[b]Return flow case only.

article, all of these benchmarks were designed to run on modest computer resources (e.g., a laptop or a single compute core) and take at most a few minutes to complete. This is true for all the codes compared here. A comprehensive timing comparison would be interesting but would require compiling all the codes on a single machine under a single architecture and operating system. As some of the codes are currently only available on one platform (e.g., Windows or Linux), this effort as not yet been undertaken at this stage of the intercomparison project.

4.1. Infiltration Excess

In this test case, infiltration excess (Hortonian) runoff is produced by ensuring that surface saturation and ponding occur before complete saturation of the soil column. This is achieved by specifying a K_s smaller than the rainfall rate. The simulations are reported for different values of K_s as given in Table 3, noting that the higher K_s value will yield more infiltration than the lower value. The domain used is a simple, one-dimensional hillslope shown in Figure 1, with a uniform soil depth of 5 m and a no-flow bottom boundary representing an impermeable base. A rainfall event 200 min in duration with a rate of 3.3 $\times 10^{-4}$ m/min was applied to generate runoff, followed by 100 min of recession.
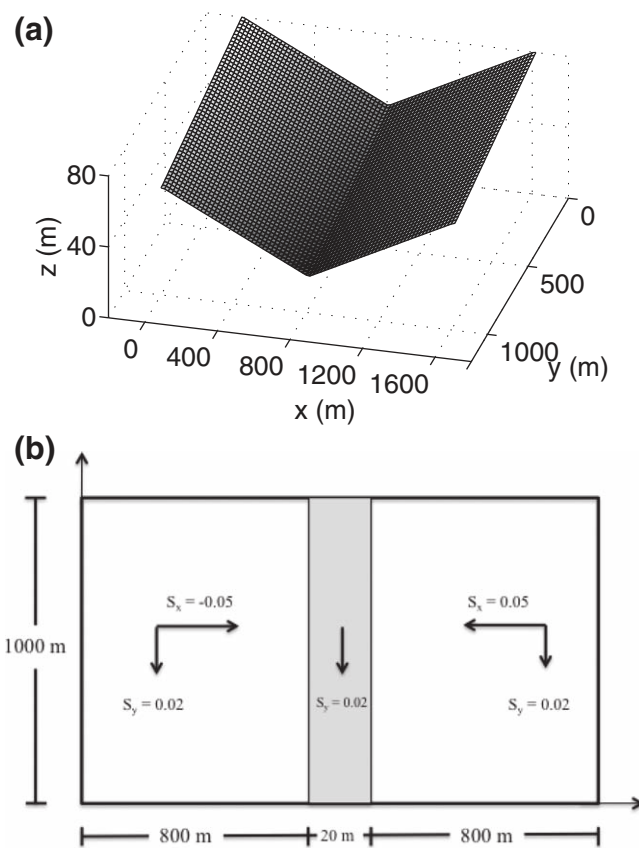
4.2. Saturation Excess

For the saturation excess test case, we use the same hillslope as the previous test case. However, in this benchmark, saturation excess (Dunne) runoff is produced by ensuring complete saturation of the soil column and intersection of the water table with the land surface. This is achieved by specifying a hydraulic conductivity larger than the rainfall rate. Two simulations are reported, for different values of initial water table depth as given in Table 3. As in the infiltration excess case, rainfall is applied for 200 min at a rate of 3.3 $\times 10^{-4}$ m/min with an additional 100 min of recession.

Figure 1. Domain for the infiltration excess, saturation excess, and return flow test cases [after *Sulis et al.*, 2010].

4.3. Tilted V-Catchment

The tilted V-catchment [*Gottardi and Venutelli*, 1993; *Panday and Huyakorn*, 2004; *Kollet and Maxwell*, 2006; *Sulis et al.*, 2010] is formed by the union of two inclined planar rectangles of width 800 m and length 1000 m connected together by a 20 m wide sloping channel (Figure 2). This test case is used to assess the behavior of the surface routing component of the various codes without any contribution from the subsurface by assuming that no infiltration occurs. The simulation consists of a 90 min rainfall event (at a uniform intensity of 1.8×10^{-4} m/min) followed by 90 min of drainage.

4.4. Slab

The slab case (first introduced in *Kollet and Maxwell* [2006]) involves a simple one-dimensional hillslope with a heterogeneous subsurface. Previous studies have demonstrated that spatial heterogeneity of subsurface hydraulic properties has a significant influence on runoff generation. In this series of simulations, the subsurface is uniform (with a K_s value of 6.94×10^{-4} m/min) except for a very low conductivity slab ($K_s = 6.94 \times 10^{-6}$ m/min) at the sur-
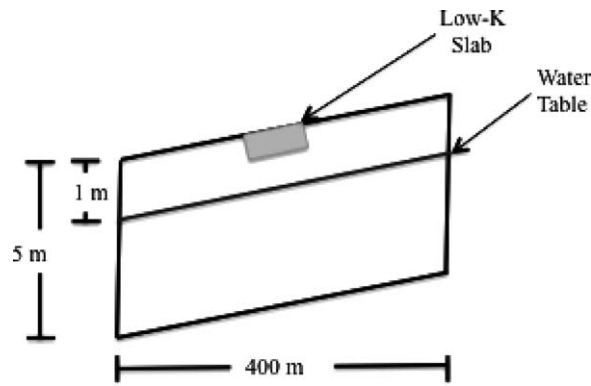

(a)

(b)

$S_x = -0.05$ $S_x = 0.05$

$S_y = 0.02$ $S_y = 0.02$ $S_y = 0.02$

1000 m

800 m   20 m   800 m

Figure 2. Tilted V-catchment domain for overland and channel flow tests [after *Kollet and Maxwell*, 2006; *Sulis et al.*, 2010]. S_x and S_y are slope inclinations in the x and y directions, respectively.

face of thickness 0.05 m situated midway along the hillslope (Figure 3). The saturated hydraulic conductivity of the slab is designed to generate infiltration excess runoff while the hydraulic conductivity of the rest of the domain is large and will only generate runoff through saturation excess. The problem setup is shown in Figure 3.

4.5. Return Flow

This test case uses the same hillslope domain as for the infiltration and saturation excess tests and is shown in Figure 1. Return flow is generated by an atmospheric forcing sequence formed by an initial 200 min rainfall event of uniform intensity of 1.5×10^{-4} m/min followed by 200 min of evaporation at a uniform rate of 5.4×10^{-6} m/min. All the models are run with a uniform discretization comprising 100 vertical layers. Two hillslope inclinations are considered (0.5% and 5%) to highlight the effects of the different characteristic time scales of the surface and subsurface processes.

5. Results and Discussion

5.1. Infiltration Excess

The results of the infiltration excess test case for all models is shown in Figure 4 and summary metrics are given in Table 4. The outflow as a function of time is plotted in this figure. We can see that in general all models show good agreement, exhibiting very similar behavior throughout all phases of the hydrograph and predicting very similar runoff amounts. Peak outflows differ by less than 3% across all models (Table 4) while peak discharge times differ by approximately 1% for the higher K_s case. The disagreement between models is greatest in the prediction of time to reach steady state (as defined by an outflow rate greater than 95% of the value at 200 min) for the lower K_s case with a maximum difference of approximately 20%, with tRIBS + VEGGIE predicting the earliest arrival and ParFlow, CATHY, OGS, and HGS grouped closely with the latest arrival. The

Figure 3. Domain for the slab test case.

maximum difference between models during the recession curve was approximately 30%, evaluated as a difference between discharge at 250 min of simulation time between HGS and tRIBS + VEGGIE. We see that the models agree more closely for the larger of the two K_s values, with differences in the recession of approximately 60% (again calculated at $t = 250$ min). Overall, four of the models (Par-Flow, CATHY, OGS, and HGS) appear to cluster the closest together, particularly during the rising limb and in the prediction of time to steady state. These models are similar in coupling strategy, which might explain these results, particularly for the lower K_s case.

5.2. Saturation Excess

Figure 5 shows the outflow rates for the seven models at initial water table depths $wt = 0.5$ and 1.0 m. Summary metrics are again given in Table 4. The maximum difference in total outflow rate is 12% (measured between the CATHY and tRIBS + VEGGIE models) for the $wt = 1.0$ m case at $t = 200$ min. Note that while the difference in outflow rate is 14% the difference in cumulative outflow is 15% (again between CATHY and tRIBS + VEGGIE) for the $wt = 1.0$ m case. For both water table configurations, initiation of ponding, at which discharge is first seen in the plots and which also corresponds to the peak flow, occurs at about the same time for all seven models (differences of approximately 1%, Table 4). The HGS model predicts the fastest change in the rising limb of the hydrograph at the onset of outflow, with a change in convexity at early times. Note that the HGS model shares a surface flow formulation with that presented by *Gottardi and Venutelli* [1993] where results (e.g., Figure 4 of that reference) also show very similar behavior for surface flow. The CATHY and PAWS models have the slowest increase in slope in the initial portion of the rising limb, and the CATHY model maintains, overall during the rising limb, a lower outflow rate at any given time,
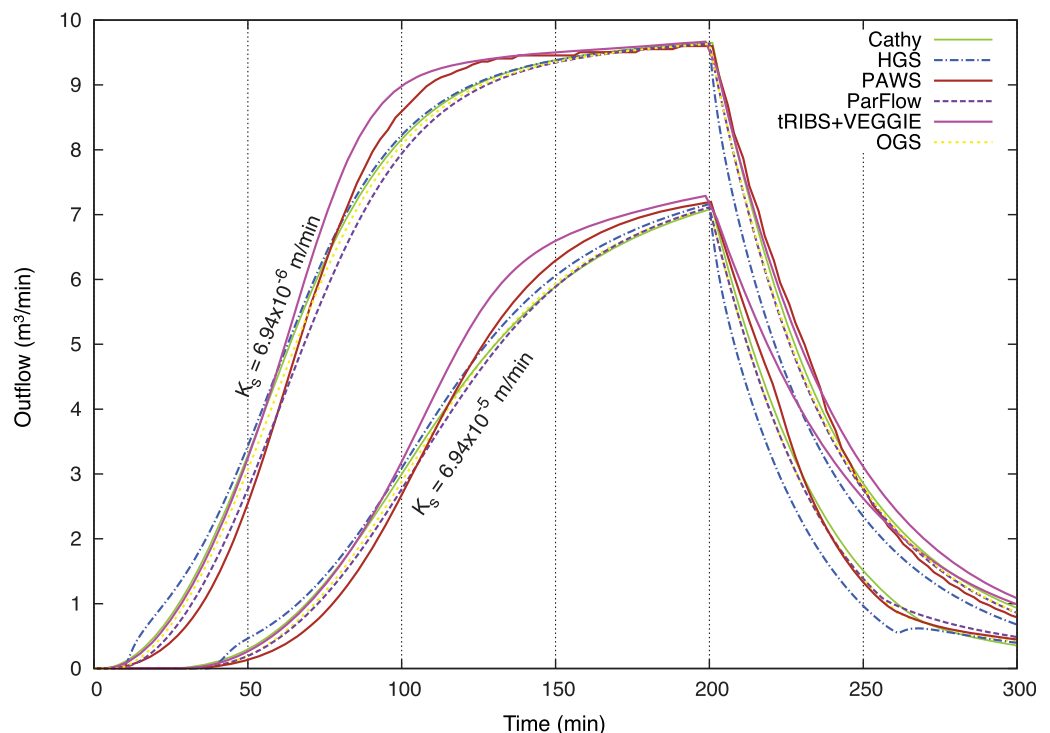

Figure 4. Simulation results for the infiltration excess test case using two different values of saturated hydraulic conductivity K_s.

Table 4. Summary Metrics for Selected Cases by Model[a]

| | Summary Metrics for Each Case | | | | | | | | |
| | Infiltration Excess $K_s = 0.1$ | | Saturation Excess $wt = 1.0$ | | Tilted V-Catchment | | Slab Case | | |
	Qpeak	tpeak	Qpeak	tpeak	Qpeak	tpeak	Qpeak	tpeak	tslab
CATHY	7.0920	201	8.8200	200	291.6000	84	1.0878	200	121.02
HGS	7.1640	200	9.4320	200	291.5400	90	1.1586	200	121.8
PIHM					291.6000	88	1.0926	200.0	127
ParFlow	7.1100	200	9.3060	200	291.9600	83	1.1580	198	114.4
PAWS	7.1940	200.5	9.8640	200.5	288.0000	90	1.2420	200.1	111.8
OGS	7.1040	200	9.2100	197.3	291.9600	68.33	1.2060	199.8	114.3
tRIBS + VEGGIE	7.2900	198.75	10.2060	198.75	291.5400	90	1.2480	199.7	79.7

[a]Qpeak is the peak flow in m³/min, tpeak is the time of peak flow in min, and tslab is the average onset of flow due to the slab.

corresponding to higher infiltration rates. The PAWS and tRIBS + VEGGIE models show a small overshoot for the $wt = 0.5$ m case with an outflow rate 0.1% larger than steady state (tRIBS + VEGGIE) and 0.7% (PAWS). Both PAWS and tRIBS + VEGGIE display a similar receding limb for the $wt = 0.5$ and 1.0 m cases.

5.3. Tilted V-Catchment

The outflow results of the tilted V-catchment case are shown in Figure 6 and summary metrics are given in Table 4. All models predict generally similar behavior, with the greatest differences occurring between OGS and ParFlow in the prediction of time to steady state, approximately 25% (as defined by an outflow rate greater than 95% of the value at 90 min) and between OGS and PAWS in prediction of flow rate, approximately 2%. There is greater model agreement during the recession phase of the hydrograph than during the rising limb phase. While the differences between the seven models are greater for this V-catchment test case than for the previous sloping plane tests, owing to greater complexity of the simulation domain and to the different overland and channel routing models used, they are significantly less that those reported in *Panday and Huyakorn* [2004] for a suite of standard overland flow watershed models.
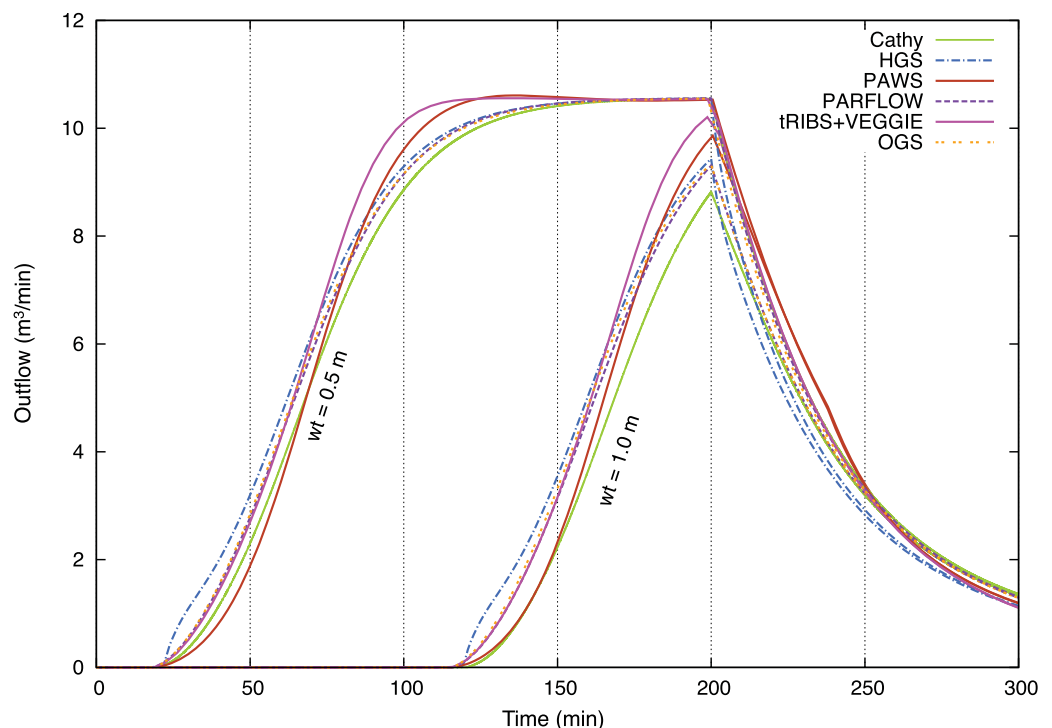
Figure 5. Simulation results for the saturation excess test case using two different values of initial water table depth *wt*.
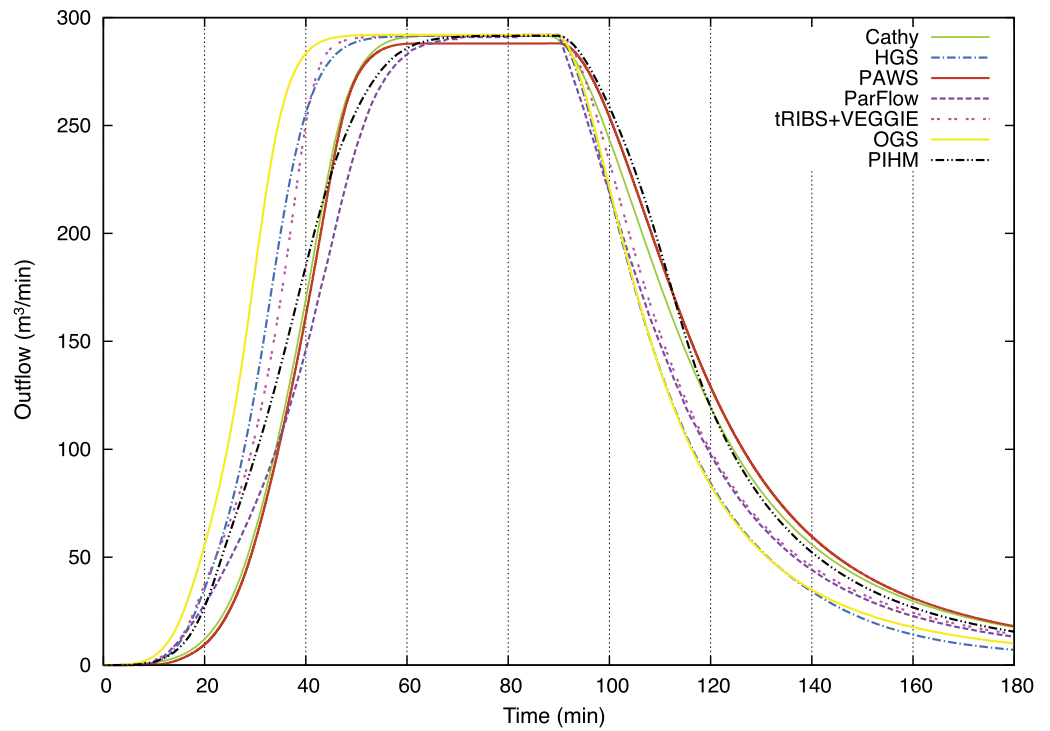
Figure 6. Simulation results for the tilted V-catchment test case.

5.4. Slab

The outflow results of the slab test case are shown in Figure 7 again with summary metrics in Table 4. While all models represent the same basic features created by the inclusion of the low-K_s slab, significant differences appear in the details of these results. The largest model differences are in the prediction of the onset of
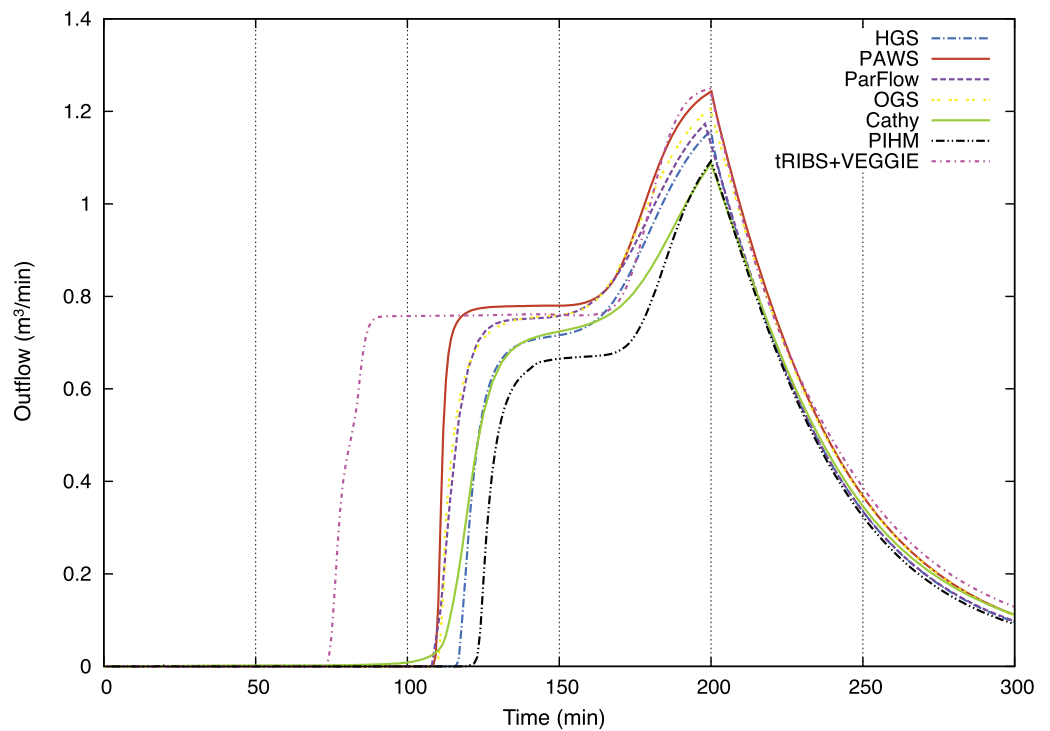

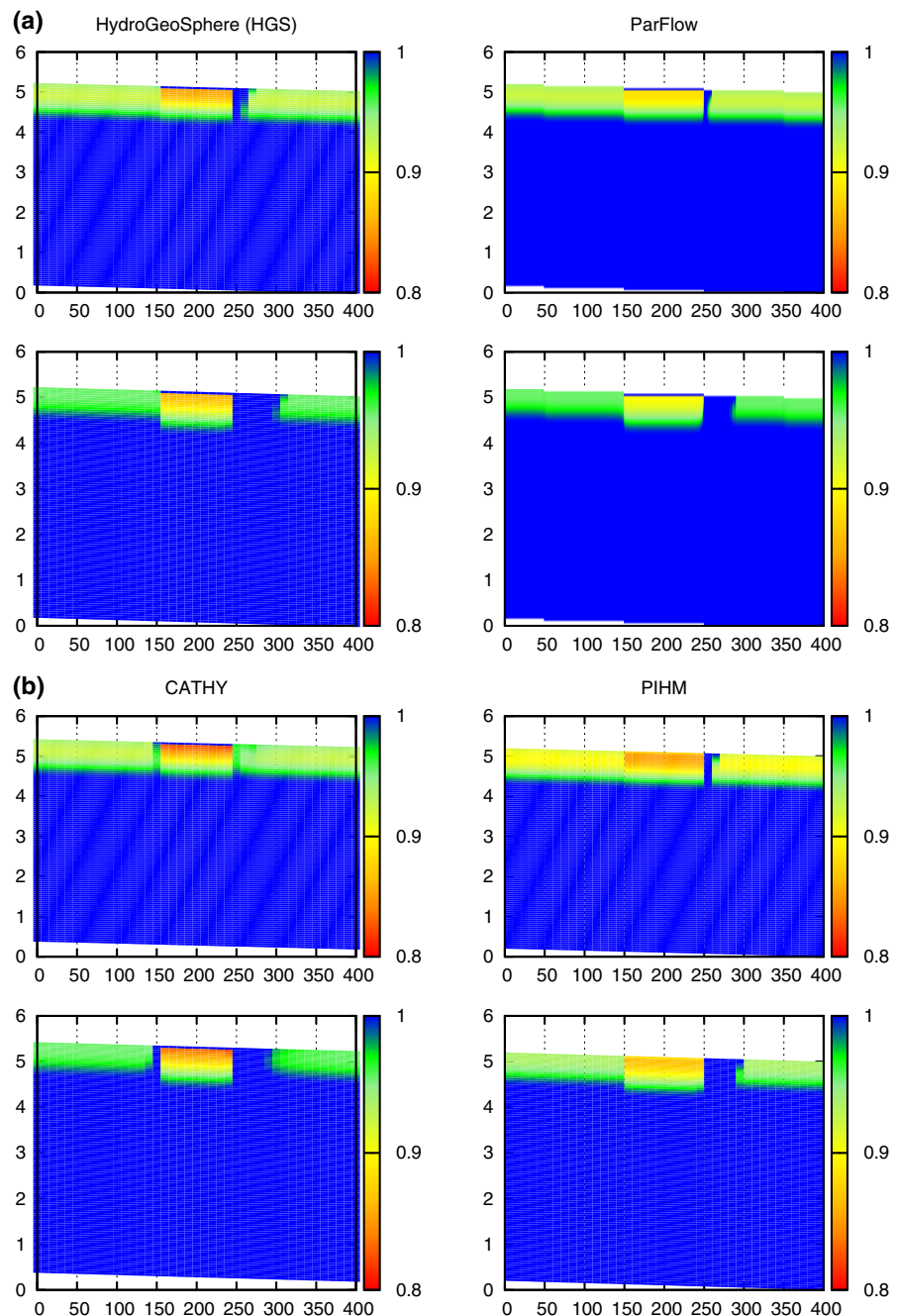**Figure 7.** Outflow results for the slab test case.

Figure 8. Saturation profiles for the slab test case at times 60 and 90 min (top and bottom graphs, respectively, for each model).

flow, with tRIBS + VEGGIE predicting flow at 75 min and PIHM predicting flow at 125 min. There are also significant differences in the predicted peak flow although these are very similar to the difference in the "plateau" of quasi-steady flow created by the slab. The recession period is where model agreement is closest. Two reduced-dimensionality models appear to group closely together (PAWS and tRIBS + VEGGIE) in peak flow but not onset time, where PAWS and ParFlow appear to be in close agreement. The CATHY model appears most diffusive, particularly at early times. This behavior has been discussed in *Sulis et al.* [2010]. Par-Flow, OGS, and HGS group quite closely together, particularly ParFlow and OGS, and all three at the time of peak flow, as do the results from CATHY and PIHM. We might note that both ParFlow and OGS are run using a structured configuration and this might contribute to their close agreement, and similarly for CATHY and PIHM, which are both unstructured codes.
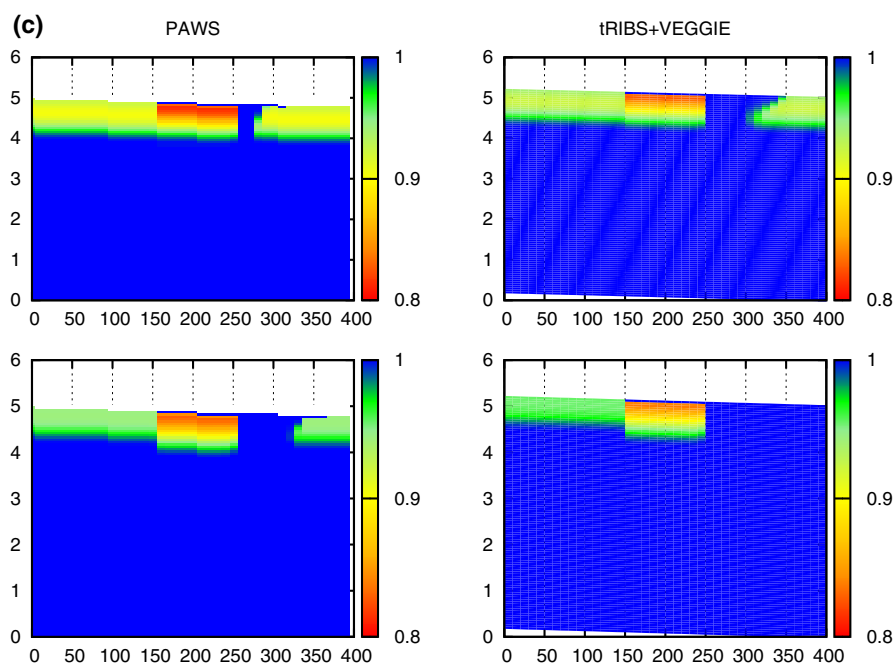
Figure 8. (continued)

Figure 8 plots snapshots of saturation at two points in time (60 and 90 min) for six of the seven models. These times are before the onset of outflow and diagnose model behavior in a manner not immediately apparent from the hydrograph alone. It should be noted that this problem presents very complex physical processes, with runoff, run-on, concentrated infiltration, and lateral unsaturated flow playing important roles in overall system behavior. In this figure, significant saturation differences are seen across all models. Three models that use globally implicit solution strategies (PIHM, ParFlow, and HGS) appear to show the greatest similarity in saturation at both times. Differences in saturation at the end of the slab simulation are important for longer, multievent time series. Because the slab case simulated here is a single storm, the final saturation would represent the initial saturation for subsequent hyetographs. The differences between models seen here in Figure 8 may likely be amplified for multiple stress period simulations.

5.5. Return Flow

The return flow case, run for two different slopes, produces the greatest model disagreement. The results of this test case are shown in Figure 9 and are plotted as the intersection point between the water table and the land surface as a function of time. We see that the water table very quickly intersects the ground surface (generating runoff) and rises very far up the hillslope to reach a quasi-steady equilibrium, before recessing back down to the hillslope outlet. In general all models predict this basic behavior for both slopes. However, the models vary widely in their prediction of the water table-ground surface intersection as a function of time.

This is a highly nonlinear test problem and not surprisingly the results between models are the most disparate. For the 0.5% rising limb ParFlow, CATHY, PAWS, and OGS all group closely together. All codes are surprisingly similar in their prediction of time at steady state for this case. The recession for most codes is bracketed for the most part by CATHY's rill and sheet flow formulations, a result seen previously for a ParFlow/CATHY comparison [*Sulis et al.*, 2010]. tRIBS + VEGGIE produces a very fast recession of the water table, which might be related to the one-dimensional treatment of the unsaturated zone. PAWS exhibits good agreement with ParFlow for both 5% and 0.5% slopes, which is interesting as it highlights agreement between two different numerical approaches (asynchronous linking compared to fully implicit). It should also be noted that the 1-D unsaturated zone formulation in PAWS can approximate the water table location for most of the recession. For the 5% slope, we do see a disagreement between the simulations. We no longer see a similar prediction of steady state time (differences are approximately 50%) and the rill/sheet flow formulations of CATHY no longer bracket the suite of simulation results.
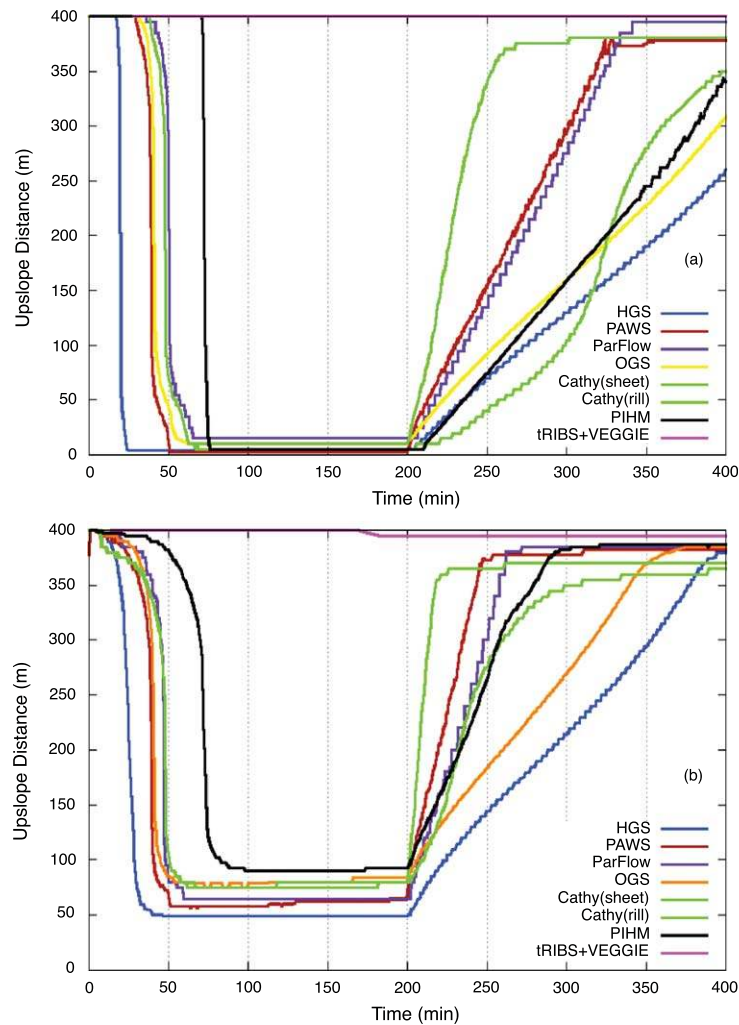
Figure 9. Simulation results for the return flow test case using hillslope inclinations of (a) 0.5% and (b) 5%. Note that the upslope distance represents the intersection point between the water table and the land surface and is plotted here as a function of time.

5.6. Summary Discussion

When one looks at the results in Table 4 the peak flow rate and peak timing metrics are quite consistent across all codes for the three more simple test cases. We see more disagreement between the models for the slab and return flow cases. These differences point to combined runoff/run-on mechanisms as being highly nonlinear and particularly challenging to solve. For runoff cases with simple infiltration, the model agreement is quite good. However, cases that have strong unsaturated dynamics and large fluctuations in water table (particularly tied to runoff) appear to be much more challenging to capture. These runoff processes are quite important in scaling and capturing groundwater-surface water exchange, having significant implications for larger areas and longer simulation times. Furthermore, we see a grouping between the implicit codes and asychronous linking codes. For the simple cases, asynchronously linked codes predict more outflow and thus less subsurface storage compared to the iterative or globally implicit codes.

6. Conclusions

In this paper, seven integrated hydrologic models were intercompared using a standard set of test problems. The models represent a range of coupling strategies and solution techniques. In general, all the models perform similarly on the test cases simulated. In particular, all models agree very closely for the infiltration excess, saturation excess, and tilted V-catchment cases. The more complex cases, slab and return flow, resulted in some significant differences in model behavior. We draw some specific conclusions from this work:

1. Model agreement is good for the simpler test cases. These cases, particularly those with purely surface flow (tilted V), 1-D infiration (infiltration excess, specifically for the larger K_s value), and less complex water table dynamics (saturation excess) generally have small model differences (5% or less). These cases cover a large range of classical (yet not overly complex) runoff generating mechanisms often encountered in catchment hydrology and can serve to build model confidence.

2. Model disagreement is large for the test cases representing more complex runoff/run-on processes (particularly the slab case) and rapid water table dynamics (return flow case), and are clearly a more challenging problem to solve. Here we see model results grouping by dimensionality and by solution technique. These cases represent somewhat more recently identified runoff generating mechanisms [e.g., *Woolhiser et al.*, 1996; *Maxwell and Kollet*, 2008b; *Meyerhoff and Maxwell*, 2011] where heterogeneity and more complex saturated flow contribute substantially [e.g., *Loague et al.*, 2010]. They can pose challenges, for instance, in upscaling for parameterization in large-scale models [e.g., *Liang et al.*, 1996].

3. Though we see *quantitative differences* between model results for the more complex cases, we also see *qualitative agreement*. We see the same behavior in all models for a range of challenging test problems. This provides confidence in all of the models included in this intercomparison and an understanding of runoff generating processes where models agree well and where differences might be expected.

These cases provide a framework for model evaluation and intercomparison as the field of coupled hydrologic models advances. However, this intercomparison exercise is the first step in a continuing effort that will develop additional benchmarks that increase in complexity. These cases will include real sites (e.g., the Borden test case as presented in *Jones et al.* [2006]) and additional processes such as the land-energy balance and contaminant transport. Additional cases will increase in scale, possibly taking advantage of parallel or high performance computing in hydrology [e.g., *Kollet et al.*, 2010; *Maxwell*, 2013] to extend to high resolution and large extent. These efforts will continue to build the community of hydrologic modelers, carefully guiding scientific understanding as integrated models increase in complexity.

References

Aquanty Inc. (2013), *HGS 2013, HydroGeoSphere User Manual*, 435 pp., Waterloo, Ontario, Canada.

Ashby, S. F., and R. D. Falgout (1996), A parallel multigrid preconditioned conjugate gradient algorithm for groundwater flow simulations, *Nucl. Sci. Eng.*, *124*(1), 145–159.

Bear J. (1979), *Hydraulics of Groundwater*, McGraw-Hill, New York.

Bixio, A. C., G. Gambolati, C. Paniconi, M. Putti, V. M. Shestopalov, V. N. Bublias, A. S. Bohuslavsky, N. B. Kastelteseva, and Y. F. Rudenko (2002), Modeling groundwater–surface water interactions including effects of morphogenetic depressions in the Chernobyl exclusion zone, *Environ. Geol.*, *42*(2–3), 162–177.

Brookfield, A. E., E. A. Sudicky, and Y.-J. Park (2008), Analysis of thermal stream loadings in a fully-integrated surface/subsurface modelling framework, *IAHS Publ. 321*, pp. 117–123.

Brooks, R. H., and A. T. Corey (1964), Hydraulic properties of porous media, *Hydrol. Pap. 3*, Colo. State Univ., Fort Collins.

Camporese, M., C. Paniconi, M. Putti, and P. Salandin (2009), Ensemble Kalman filter data assimilation for a process-based catchment scale model of surface and subsurface flow, *Water Resour. Res.*, *45*, W10421, doi:10.1029/2008WR007031.

Camporese, M., C. Paniconi, M. Putti, and S. Orlandini (2010), Surface-subsurface flow modeling with path-based runoff routing, boundary condition-based coupling, and assimilation of multisource observation data, *Water Resour. Res.*, *46*, W02512, doi:10.1029/2008WR007536.

Cardenas, M. B. (2008a), The effect of river bend morphology on flow and timescales of surface water-groundwater exchange across point-bars, *J. Hydrol.*, *362*(1–2), 134–141, doi:10.1016/j.jhydrol.2008.08.018.

Cardenas, M. B. (2008b), Surface water-groundwater interface geomorphology leads to scaling of residence times, *Geophys. Res. Lett.*, *35*, L08402, doi:10.1029/2008GL033753.

Cardenas, M. B., and M. N. Gooseff (2008), Comparison of hyporheic exchange under covered and uncovered channels based on linked surface and groundwater flow simulations, *Water Resour. Res.*, *44*, W03418, doi:10.1029/2007WR006506.

Cardenas, M. B., J. L. Wilson, and R. Haggerty (2008), Residence time of bedform-driven hyporheic exchange, *Adv. Water Resour.*, *31*(10), 1382–1386, doi:10.1016/j.advwatres.2008.07.006.

Celia, M. A., E. T. Bouloutas, and R. L. Zarba (1990), A general mass-conservative numerical solution for the unsaturated flow equation, *Water Resour. Res.*, *26*(7), 1483–1496, doi:10.1029/WR026i007p01483.

Chen, T. H., et al. (1997), Cabauw experimental results from the Project for Intercomparison of land-surface parameterizations schemes, *J. Clim.*, *10*, 1194–1215.

Condon, L. E., and R. M. Maxwell (2013), Implementation of a linear optimization water allocation algorithm into a fully integrated physical hydrology model, *Adv. Water Resour.*, *60*, 135–147, doi:10.1016/j.advwatres.2013.07.012.

Dagès, C., C. Paniconi, and M. Sulis (2012), Analysis of coupling errors in a physically-based integrated surface water–groundwater model, *Adv. Water Resour.*, *49*, 86–96, doi:10.1016/j.advwatres.2012.07.019.

Dawson, C. (2008), A continuous/discontinuous Galerkin framework for modeling coupled subsurface and surface water flow, *Comput. Geosci.*, *12*, 451–472, doi:10.1007/s10596-008-9085-y.

Delfs, J.-O., C.-H. Park, and O. Kolditz (2009), A sensitivity analysis of Hortonian flow, *Adv. Water Resour.*, *32*(9), 1386–1395, doi:10.1016/j.advwatres.2009.06.005.

Delfs, J.-O., F. Blumensaat, E. W. Wang, P. Krebs, and O. Kolditz (2012), Coupling hydrogeological with surface runoff model in a Poltva case study in Western Ukraine, *Environ. Earth Sci.*, *65*, 1439–1457, doi:10.1007/s12665-011-1285-4.

Delfs, J.-O., W. Wang, W. T. Kalbacher, A. K. Singh, and O. Kolditz (2013), A coupled surface/subsurface flow model accounting for air entrapment and air pressure counterflow, *Environ. Earth Sci.*, *69*(2), 395–414, doi:10.1007/s12665-013-2420-1.

Ebel, B. A., and K. Loague (2008), Rapid simulated hydrologic response within the variably saturated near surface, *Hydrol. Processes*, *22*(3), 464–471, doi:10.1002/hyp.6926.

Ebel, B. A., K. Loague, J. E. VanderKwaak, W. E. Dietrich, D. R. Montgomery, R. Torres, and S. P. Anderson (2007), Near-surface hydrologic response for a steep, unchanneled catchment near Coos Bay, Oregon. 2: Physics-based simulations, *Am. J. Sci.*, *307*(4), 709–748, doi: 10.2475/04.2007.03.

Ebel, B. A., K. Loague, D. R. Montgomery, and W. E. Dietrich (2008), Physics-based continuous simulation of long-term near-surface hydrologic response for the Coos Bay experimental catchment, *Water Resour. Res.*, *44*, W07417, doi:10.1029/2007WR006442.

Ebel, B. A., B. B. Mirus, C. S. Heppner, J. E. VanderKwaak, and K. Loague (2009), First-order exchange coefficient coupling for simulating surface water-groundwater interactions: Parameter sensitivity and consistency with a physics-based approach, *Hydrol. Processes*, *23*(13), 1949–1959, doi:10.1002/Hyp.7279.

Ferguson, I. M., and R. M. Maxwell (2010), The role of groundwater in watershed response and land surface feedbacks under climate change, *Water Resour. Res.*, *46*, W00F02, doi:10.1029/2009WR008616.

Freeze, R. A., and R. L. Harlan (1969), Blueprint for a phyiscally-based, digitally-simulated hydrologic response model, *J. Hydrol.*, *9*, 237–258.

Frei, S., J. H. Fleckenstein, S. J. Kollet, and R. M. Maxwell (2009), Patterns and dynamics of river-aquifer exchange with variably-saturated flow using a fully-coupled model, *J. Hydrol.*, *375*(3–4), 383–393, doi:10.1016/J.Jhydrol.2009.06.038.

Furman, A. (2008), Modeling coupled surface–subsurface flow processes: A review, *Vadose Zone J.*, *7*(2), 741–756, doi:10.2136/vzj2007.0065.

Gauthier, M.-J., M. Camporese, C. Rivard, C. Paniconi, and M. Larocque (2009), A modeling study of heterogeneity and surface water-groundwater interactions in the Thomas Brook catchment, Annapolis Valley (Nova Scotia, Canada), *Hydrol. Earth Syst. Sci.*, *13*, 1583–1596, doi:10.5194/hess-13-1583-2009.

Gottardi, G., and M. Venutelli (1993), A control-volume finite-element model for two-dimensional overland flow, *Adv. Water Resour.*, *16*(5), 277–284, doi:10.1016/0309-1708(93)90019-C.

Guay, C., M. Nastev, C. Paniconi, and M. Sulis (2013), Comparison of two modeling approaches for groundwater–surface water interactions, *Hydrol. Processes*, *27*(16), 2258–2270, doi:10.1002/hyp.9323.

Gunduz, O., and M. M. Aral (2003), Simultaneous solution of coupled surface water/groundwater flow systems, in *River Basin Management II*, edited by C.A. Brebbia, pp. 25–33, Canary Islands, Spain.

Gunduz, O., and M. M. Aral (2005), River networks and groundwater flow: A simultaneous solution of a coupled system, *J. Hydrol.*, *301*(1–4), 216–234, doi:10.1016/j.jhydrol.2004.06.034.

Henderson-Sellers, A., A. J. Pitman, P. K. Love, P. Irannejad, and T. H. Chen (1995), The Project for Intercomparison of Land Surface Parameterization Schemes (PILPS): Phase 2 and 3, *Bull. Am. Meteorol. Soc.*, *76*, 489–503, doi:10.1175/1520-0477.

Heppner, C., and K. Loague (2008), A dam problem: Simulated upstream impacts for a searsville like watershed, *Ecohydrology*, *1*(4), 408–424, doi:10.1002/eco.34.

Heppner, C. S., Q. Ran, J. E. VanderKwaak, and K. Loague (2006), Adding sediment transport to the integrated hydrology model (InHM): Development and testing, *Adv. Water Resour.*, *29*(6), 930–943, doi:10.1016/j.advwatres.2005.08.003.

Heppner, C. S., K. Loague, and J. E. VanderKwaak (2007), Long-term InHM simulations of hydrologic response and sediment transport for the R-5 catchment, *Earth Surf. Processes Landforms*, *32*(9), 1273–1292, doi:10.1002/esp.1474.

Hunt, R. J., D. E. Prudic, J. F. Walker, and M. P. Anderson (2008), Importance of unsaturated zone flow for simulating recharge in a humid climate, *Ground Water*, *46*(4), 551–560, doi:10.1111/j.1745-6584.2007.00427.x.

Ivanov, V. Y., E. R. Vivoni, R. L. Bras, and D. Entekhabi (2004), Catchment hydrologic response with a fully distributed triangulated irregular network model, *Water Resour. Res.*, *40*, W11102, doi:10.1029/2004WR003218.

Ivanov, V. Y., R. L. Bras, and E. R. Vivoni (2008), Vegetation-hydrology dynamics in complex terrain of semiarid areas. I: A mechanistic approach to modeling dynamic feedbacks, *Water Resour. Res.*, *44*, W03429, doi:10.1029/2006WR005588.

Ivanov, V. Y., S. Fatichi, G. D. Jenerette, J. F. Espeleta, P. A. Troch, and T. E. Huxman (2010), Hysteresis of soil moisture spatial heterogeneity and the ''homogenizing'' effect of vegetation, *Water Resour. Res.*, *46*, W09521, doi:10.1029/2009WR008611.

Jones, J. E., and C. S. Woodward (2001), Newton-Krylov-multigrid solvers for large-scale, highly heterogeneous, variably saturated flow problems, *Adv. Water Resour.*, *24*(7), 763–774, doi:10.1016/S0309-1708(00)00075-0.

Jones, J. P., E. A. Sudicky, A. E. Brookfield, and Y. J. Park (2006), An assessment of the tracer-based approach to quantifying groundwater contributions to streamflow, *Water Resour. Res.*, *42*, W02407, doi:10.1029/2005WR004130.

Jones, J. P., E. A. Sudicky, and R. G. McLaren (2008), Application of a fully-integrated surface-subsurface flow model at the watershed-scale: A case study, *Water Resour. Res.*, *44*, W03407, doi:10.1029/2006WR005603.

Kim, J., A. Warnock, V. Y. Ivanov, and N. D. Katopodes (2012), Coupled modeling of hydrologic and hydrodynamic processes including overland and channel flow, *Adv. Water Resour.*, *37*, 104–126, doi:10.1016/j.advwatres.2011.11.009.

Kim, J. A., V. Y. Ivanov, and N. D. Katopodes (2013), Modeling erosion and sedimentation coupled with hydrological and overland flow processes at the watershed scale, *Water Resour. Res.*, *49*, 5134–5154, doi:10.1002/wrcr.20373.

Kolditz, O., et al. (2012), OpenGeoSys: An open-source initiative for numerical simulation of thermo-hydro-mechanical/chemical (THM/C) processes in porous media, *Environ. Earth Sci.*, *67*(2), 589–599.

Kollet, S. J., and R. M. Maxwell (2006), Integrated surface-groundwater flow modeling: A free-surface overland flow boundary condition in a parallel groundwater flow model, *Adv. Water Resour.*, *29*(7), 945–958, doi:10.1016/j.advwatres.2005.08.006.

Kollet, S. J., and R. M. Maxwell (2008a), Capturing the influence of groundwater dynamics on land surface processes using an integrated, distributed watershed model, *Water Resour. Res.*, *44*, W02402, doi:10.1029/2007WR006004.

Kollet, S. J., and R. M. Maxwell (2008b), Demonstrating fractal scaling of baseflow residence time distributions using a fully-coupled groundwater and land surface model, *Geophys. Res. Lett.*, *35*(7), L07402, doi:10.1029/2008GL033215.

Kollet, S. J., R. M. Maxwell, C. S. Woodward, S. Smith, J. Vanderborght, H. Vereecken, and C. Simmer (2010), Proof of concept of regional scale hydrologic simulations at hydrologic resolution utilizing massively parallel computer resources, *Water Resour. Res.*, *46*, W04201, doi:10.1029/2009WR008730.

Kumar, M., C. J. Duffy, and K. M. Salvage (2009), A second order accurate, finite volume based, integrated hydrologic modeling (fihm) framework for simulation of surface and subsurface flow, *Vadose Zone J.*, *8*(4), 873–890.

Langevin, C., E. Swain, and M. Wolfert (2005), Simulation of integrated surface-water/ground-water flow and salinity for a coastal wetland and adjacent estuary, *J. Hydrol.*, *314*(1–4), 212–234, doi:10.1016/j.jhydrol.2005.04.015.

Lemieux, J. M., E. A. Sudicky, W. R. Peltier, and L. Tarasov (2008), Dynamics of groundwater recharge and seepage over the Canadian land-scape during the wisconsinian glaciation, *J. Geophys. Res.*, *113*, F01011, doi:10.1029/2007JF000838.

Leopold, L. B., and T. Maddock Jr. (1953), The hydraulic geometry of stream channels and some physiographic implications, *Prof. Pap. 252*, U.S. Geol. Surv., Washington, D. C.

Li, Q., A. J. A. Unger, E. A. Sudicky, D. Kassenaar, E. J. Wexler, and S. Shikaze (2008), Simulating the multi-seasonal response of a large-scale watershed with a 3D physically-based hydrologic model, *J. Hydrol.*, *357*(3–4), 317–336, doi:10.1016/j.jhydrol.2008.05.024.

Li, S., and C. J. Duffy (2011), Fully coupled approach to modeling shallow water flow, sediment transport, and bed evolution in rivers, *Water Resour. Res.*, *47*, W03508, doi:10.1029/2010WR009751.

Liang, X., E. F. Wood, and D. P. Lettenmaier (1996), Surface soil parameterization of the VIC-2L model: Evaluation and modification, *Global Planet. Change*, *13*, 195–206.

Liang, X., et al. (1998), The Project for Intercomparison of Land-surface Parameterization Schemes PILPS/phase 2c/Red-Arkansas River basin experiment. 2: Spatial and temporal analysis of energy fluxes, *Global Planet. Change*, *19*, 137–159.

Loague, K., C. S. Heppner, R. H. Abrams, A. E. Carr, J. E. VanderKwaak, and B. A. Ebel (2005), Further testing of the integrated hydrology model (inhm): Event-based simulations for a small rangeland catchment located near Chickasha, Oklahoma, *Hydrol. Processes*, *19*(7), 1373–1398, doi:10.1002/hyp.5566.

Loague, K., C. S. Heppner, B. A. Ebel, and J. E. VanderKwaak (2010), The quixotic search for a comprehensive understanding of hydrologic response at the surface: Horton, Dunne, Dunton, and the role of concept-development simulation, *Hydrol. Processes*, *24*, 2499–2505, doi: 10.1002/hyp.7834.

Luo, L., et al. (2003), Effects of frozen soil on soil temperature, spring infiltration, and runoff: Results from the PILPS 2(d) Experiment at Val-dai, Russia, *J. Hydrometeorol.*, *4*, 334–351.

Markstrom, S., R. Niswonger, R. Regan, D. Prudic, and P. Barlow (2008), GSFlow-Coupled Ground-Water and Surface-Water Flow Model Based on the Integration of the Precipitation-Runoff Modeling System (PRMS) and the Modular Ground-Water Flow Model (Modflow-2005), *U.S. Geol. Surv. Tech. Methods, 6-d1*, Reston, Va., 240 pp.

Maxwell, R. M. (2013) A terrain-following grid transform and preconditioner for parallel, large-scale, integrated hydrologic modeling, *Adv. Water Resour.*, *53*, 109–117, doi:10.1016/j.advwatres.2012.10.001.

Maxwell, R. M., and N. L. Miller (2005), Development of a coupled land surface and groundwater model, *J. Hydrometeorol.*, *6*(3), 233–247, doi:10.1175/JHM422.1.

Maxwell, R. M., and S. J. Kollet (2008a), Interdependence of groundwater dynamics and land-energy feedbacks under climate change, *Nat. Geosci.*, *1*(10), 665–669, doi:10.1038/ngeo315.

Maxwell, R. M., and S. J. Kollet (2008b), Quantifying the effects of three-dimensional subsurface heterogeneity on Hortonian runoff proc-esses using a coupled numerical, stochastic approach, *Adv. Water Resour.*, *31*(5), 807–817, doi:10.1016/j.advwatres.2008.01.020.

Maxwell, R. M., F. K. Chow, and S. J. Kollet (2007), The groundwater-land-surface-atmosphere connection: Soil moisture effects on the atmospheric boundary layer in fully-coupled simulations, *Adv. Water Resour.*, *30*(12), 2447–2466, doi:10.1016/j.advwatres.2007.05.018.

Maxwell, R. M., J. D. Lundquist, J. D. Mirocha, S. G. Smith, C. S. Woodward, and A. F. B. Tompson (2011), Development of a coupled groundwater-atmospheric model, *Mon. Weather Rev.*, *139*, 96–116, doi:10.1175/2010MWR3392.

McLaren, R. G., P. A. Forsyth, E. A. Sudicky, J. E. VanderKwaak, F. W. Schwartz, and J. H. Kessler (2000), Flow and transport in fractured tuff at Yucca Mountain: Numerical experiments on fast preferential flow mechanisms, *J. Contam. Hydrol.*, *43*(3–4), 211–238, doi:10.1016/S0169-7722(00)00085-1.

Meyerhoff, S. B., and R. M. Maxwell (2011), Quantifying the effects of subsurface heterogeneity on hillslope runoff using a stochastic approach, *Hydrogeol. J.*, *19*, 1515–1530, doi:10.1007/s10040-011-0753-y.

Mirus, B. B., B. A. Ebel, K. Loague, and B. C. Wemple (2007), Simulated effect of a forest road on near-surface hydrologic response: Redux, *Earth Surf. Processes Landforms*, *32*(1), 126–142, doi:10.1002/esp.1387.

Mirus, B. B., K. Loague, J. E. VanderKwaak, S. K. Kampf, and S. J. Burges (2009), A hypothetical reality of tarrawarra-like hydrologic response, *Hydrol. Processes*, *23*(7), 1093–1103, doi:10.1002/hyp.7241.

Morita, M., and B. C. Yen (2002), Modeling of conjunctive two-dimensional surface-three-dimensional subsurface flows, *J. Hydraul. Eng.*, *128*(2), 184–200.

Niu, G.-Y., C. Paniconi, P. A. Troch, R. L. Scott, M. Durcik, X. Zeng, T. Huxman, and D. C. Goodrich (2014), An integrated modelling framework of catchment-scale ecohydrological processes: 1. Model description and tests over an energy-limited watershed, *Ecohydrology*, doi: 10.1002/eco.1362.

Orlandini, S., and G. Moretti (2009), Determination of surface flow paths from gridded elevation data, *Water Resour. Res.*, *45*, W03417, doi: 10.1029/2008WR007099.

Orlandini, S., and R. Rosso (1998), Parameterization of stream channel geometry in the distributed modeling of catchment dynamics, *Water Resour. Res.*, *34*(8), 1971–1985.

Panday, S., and P. S. Huyakorn (2004), A fully coupled physically-based spatially-distributed model for evaluating surface/subsurface flow, *Adv. Water Resour.*, *27*(4), 361–382, doi:10.1016/j.advwatres.2004.02.016.

Paniconi C., and M. Putti (1994), A comparison of Picard and Newton iteration in the numerical solution of multidimensional variably satu-rated flow problems, *Water Resour. Res.*, *30*(12), 3357–3374.

Park, Y. J., E. A. Sudicky, S. Panday, and G. Matanga (2009), Implicit sub-time stepping for solving the nonlinear equations of flow in an inte-grated surface-subsurface system, *Vadose Zone J.*, *8*(4), 825–836.

Parlange, J.-Y., C. W. Rose, and G. Sander (1981), Kinematic flow approximation of runoff on a plane: An exact analytical solution, *J. Hydrol.*, *52*, 171–176.

Peyrard, D., S. Sauvage, P. Vervier, J. M. Sanchez-Perez, and M. Quintard (2008), A coupled vertically integrated model to describe lateral exchanges between surface and subsurface in large alluvial floodplains with a fully penetrating river, *Hydrol. Processes*, *22*(21), 4257–4273, doi:10.1002/hyp.7035.

Qu, W., et al. (1998), Sensitivity of latent heat flux from PILPS land-surface schemes to perturbations of surface air temperature, *J. Atmos. Sci.*, *55*(11), 1909–1927.

Qu, Y., and C. J. Duffy (2007), A semidiscrete finite volume formulation for multiprocess watershed simulation, *Water Resour. Res.*, *43*, W08419, doi:10.1029/2006WR005752.

Ran, Q., C. S. Heppner, J. E. VanderKwaak, and K. Loague (2007), Further testing of the integrated hydrology model (inhm): Multiple-species sediment transport, *Hydrol. Processes*, *21*(11), 1522–1531, doi:10.1002/hyp.6642.

Reed, S., V. Koren, M. Smith, Z. Zhang, F. Moreda, D.-J. Seo, and DMIP Participants (2004), Overall distributed model intercomparison project results, *J. Hydrol.*, *298*(1–4), 27–60, doi:10.1016/j.jhydrol.2004.03.031.

Richards, L. A. (1931), Capillary conduction of liquids through porous mediums, *J. Appl. Phys.*, *1*(5), 318–333, doi:10.1063/1.1745010.

Schaap, M. G., and F. J. Leij (1998), Database-related accuracy and uncertainty of pedotransfer functions, *Soil Sci.*, *163*(10), 765–779.

Schoups, G., J. W. Hopmans, C. A. Young, J. A. Vrugt, W. W. Wallender, K. K. Tanji, and S. Panday (2005), Sustainability of irrigated agriculture in the San Joaquin Valley, California, *Proc. Natl. Acad. Sci. U. S. A.*, *102*(43), 15,352–15,356, doi:10.1073/pnas.0507723102.

Sebben, M. L., A. D. Werner, J. E. Liggett, D. Partington, and C. T. Simmons (2013), On the testing of fully integrated surface–subsurface hydrological models, *Hydrol. Processes*, *27*(8), 1276–1285, doi:10.1002/hyp.9630.

Shen, C., and M. S. Phanikumar (2010), A process-based, distributed hydrologic model based on a large-scale method for surface–subsurface coupling, *Adv. Water Resour.*, *33*, 1524–1541, doi:10.1016/j.advwatres.2010.09.002.

Shen, C., J. Niu, and M. S. Phanikumar (2013), Evaluating controls on coupled hydrologic and vegetation dynamics in a humid continental climate watershed using a subsurface-land surface processes model, *Water Resour. Res.*, *49*(5), 2552–2572, doi:10.1002/wrcr.20189.

Shu, C. W. (1988), Total-variation-diminishing time discretizations, *SIAM J. Sci. Stat. Comput.*, *9*(6), 1073–1084, doi:10.1137/0909073.

Smerdon, B. D., C. A. Mendoza, and K. J. Devito (2007), Simulations of fully coupled lake-groundwater exchange in a subhumid climate with an integrated hydrologic model, *Water Resour. Res.*, *43*, W01416, doi:10.1029/2006WR005137.

Smerdon, B. D., C. A. Mendoza, and K. J. Devito (2008), Influence of subhumid climate and water table depth on groundwater recharge in shallow outwash aquifers, *Water Resour. Res.*, *44*, W08427, doi:10.1029/2007WR005950.

Smith, M. B., D. J. Seo, V. I. Koren, S. M. Reed, Z. Zhang, Q. Y. Duan, F. Moreda, and S. Cong (2004), The distributed model intercomparison project (DMIP): Motivation and experiment design, *J. Hydrol.*, *298*(1–4), 4–26, doi:10.1016/j.jhydrol.2004.03.040.

Sudicky, E., J. Jones, Y.-J. Park, A. Brookfield, and D. Colautti (2008), Simulating complex flow and transport dynamics in an integrated surface-subsurface modeling framework, *Geosci. J.*, *12*(2), 107–122, doi:10.1007/s12303-008-0013-x.

Sulis, M., S. B. Meyerhoff, C. Paniconi, R. M. Maxwell, M. Putti, and S. J. Kollet (2010), A comparison of two physics-based numerical models for simulating surface water–groundwater interactions, *Adv. Water Resour.*, *33*(4), 456–467, doi:10.1016/j.advwatres.2010.01.010.

Sulis, M., C. Paniconi, C. Rivard, R. Harvey, and D. Chaumont (2011a), Assessment of climate change impacts at the catchment scale with a detailed hydrological model of surface–subsurface interactions and comparison with a land surface model, *Water Resour. Res.*, *47*, W01513, doi:10.1029/2010WR009167.

Sulis, M., C. Paniconi, and M. Camporese (2011b), Impact of grid resolution on the integrated and distributed response of a coupled surface–subsurface hydrological model for the des Anglais catchment, Quebec, *Hydrol. Processes*, *25*(12), 1853–1865, doi:10.1002/hyp.7941.

Sulis, M., C. Paniconi, M. Marrocu, D. Huard, and D. Chaumont (2012), Hydrologic response to multimodel climate output using a physically based model of groundwater/surface water interactions, *Water Resour. Res.*, *48*, W12510, doi:10.1029/2012WR012304.

Tarboton, D. (1997), A new method for the determination of flow directions and upslope areas in grid digital elevation models, *Water Resour. Res.*, *33*(2), 309–319.

Therrien, R., E. A. Sudicky, Y.-J. Park, and R. G. McLaren (2012), *HydroGeoSphere: A Three-Dimensional Numerical Modelling Describing Fully-Integrated Subsurface and Surface Flow and Transport*, User Guide, Aquanty Inc., Waterloo, Ontario, Canada.

VanderKwaak, J., and E. Sudicky (2000), Application of a physically-based numerical model of surface and subsurface water flow and solute transport, *IAHS Publ. 265*, 515–523.

VanderKwaak, J. E., and K. Loague (2001), Hydrologic-response simulations for the R-5 catchment with a comprehensive physics-based model, *Water Resour. Res.*, *37*(4), 999–1013, doi:10.1029/2000WR900272.

van Genuchten, M. T. (1980), A closed-form equation for predicting the hydraulic conductivity of unsaturated soils, *Soil Sci. Soc. Am. J.*, *44*(5), 892–908.

Weill, S., A. Mazzia, M. Putti, and C. Paniconi (2011), Coupling water flow and solute transport into a physically-based surface–subsurface hydrological model, *Adv. Water Resour.*, *34*(1), 128–136, doi:10.1016/j.advwatres.2010.10.001.

Weng, P., F. Giraud, P. Fleury, and C. Chevallier (1999), Characterising and modelling groundwater discharge in an agricultural wetland on the French Atlantic coast, *Hydrol. Earth Syst. Sci.*, *7*(1), 33–42, doi:10.5194/hess-7-33-2003.

Woolhiser, D. A., R. E. Smith, and J. V. Giraldez (1996), Effects of spatial variability of the saturated conductivity on Hortonian overland flow, *Water Resour. Res.*, *32*(3), 671–678.

Yang, Z.-L., R. E. Dickinson, A. Henderson-Sellers, and A. J. Pitman (1995), Preliminary study of spin-up processes in landsurface models with the first stage data of Project for Intercomparison of Land Surface Parameterization Schemes Phase 1(a), *J. Geophys. Res.*, *100*(D8), 16,553–16,578.